Consideration of Stribeck Diagram Parameters in the Investigation on Wear and Friction Behavior in Lubricated Sliding

Marcia Marie Maru
marciamaru@yahoo.com.br

Deniol K. Tanaka
dktanaka@usp.br
Escola Politecnica, University of São Paulo
Department of Mechanical Engineering
05508-900 São Paulo, SP. Brazil

This paper deals with an experimental study of both wear and friction responses of lubricated sliding tests, considering both responses in Stribeck diagram. Analyses concerning the wear coefficient by Archard equation were also done. Tests were oil-bath lubricated, performed through a machine with devices for rotating pin-on-disk and reciprocating pin-on-plate tests. Tested specimens were pins of AISI52100 steel and counter-bodies of AISI8640 steel. Presence of additives and contamination in lubricant oil was investigated under two mechanical loading levels, determined by the velocity/load ratio. Wear was studied by means of optical microscope and dimensional analysis of the worn surfaces. The use of a wear coefficient similar to that of Archard equation for characterizing sliding wear behavior is discussed. Differences were observed in the wear trend of the rotating and the reciprocating tests in terms of Stribeck parameters considerations.
Keywords*: wear, friction, paraffin oil, abrasive contaminant, rotating movement, reciprocating movement, mechanical loading, mixed lubrication*

Introduction

Significant number of mechanical components operates under lubricated conditions, where the main function of lubricant is the reduction of both friction and wear of the sliding parts. Advancements in oil-surface interaction understanding may allow better fundament-based selection of both lubricants and components materials. In practice, experimental approach is common to investigate these alternatives, where actual systems are simulated in laboratory. However, it is frequently seen that most of investigations disregard similarity in lubrication mode occurring in the tribometer to real system. One probable reason is that experimental investigations are mostly focused on evaluation of changes in component material; then, minor considerations are directed to the lubrication adequacy of the tribossystem. A critical point is that, depending on lubrication regime, different surface interaction mechanisms occur, certainly leading to distinct wear and friction responses. In most cases, friction and lubrication relationship is characterized with basis on ηV/W (oil viscosity x sliding velocity / normal load) factor (Wakuri et al., 1988; Wakuri et al., 1995), in a curve called Stribeck diagram, as shown in Fig. 1, reproduced from Bayer (1994).

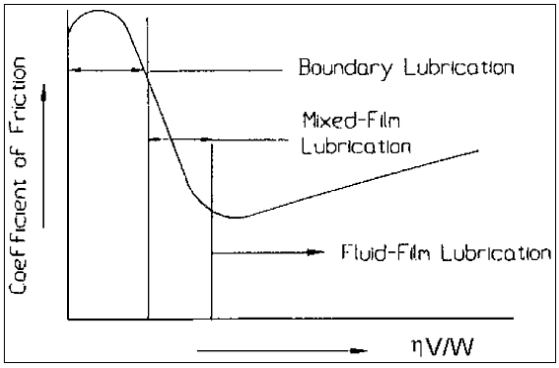

Figure 1. Schematic representation of Stribeck diagram. η: oil viscosity, V: sliding velocity, W: normal load (reproduced from Bayer, 1994).

Paper accepted July, 2006. Technical Editor: Paulo Eigi Miyagi.

Friction behavior in Stribeck diagram is used to explain rubbing phenomena occurring in lubricated contacts. For high values of ηV/W, friction coefficient is linearly ascending due to fluid film lubrication; friction is related to viscous dragging forces in the oil film. When load increases or oil viscosity and/or velocity decreases, the ηV/W factor falls. Then, the fluid film becomes thinner and, consequently, friction coefficient decreases, up to a minimum value. For even smaller values of ηV/W, fluid film thickness is further reduced, and metal-to-metal contact starts to occur. Then, friction coefficient increases as the ηV/W factor decreases. Such rise in friction coefficient is also related to oil viscosity increase in some regions at contact area under high contact pressure. These phenomena characterize the mixed lubrication regime. Further reduction in ηV/W factor makes metal-to-metal contact stronger. Film thickness becomes smaller than the height of surface asperities and then boundary lubrication regime will occur, as described by Ludema (1996).

On the other hand, in the case of two rough surfaces, several authors (Hutchings, 1992; Bayer, 1994; Neale, 1997) consider the λ value to characterize lubrication in rubbing contacts. This value is determined by the relation of oil film thickness (h) and equivalent surface roughness of both surfaces (σ). Oil film thickness h can be determined from calculations of EHL (elastohydrodynamic) film, such as those described in 1960's by Dowson and coworkers (Dowson, 1997). In terms of equivalent roughness σ, several proposals are seen for the topography parameter to be considered for σ calculation (Cheng, 1988; Hutchings, 1992; Dowson, 1995, Dowson, 1997); however, most authors still consider combination of Ra (average value of asperity height) roughness of both surfaces (Bayer, 1994).

High λ values are related to fluid film lubrication, where the solid bodies do not interact and, as mentioned by Bayer (1994), wear is small and limited by fatigue mechanisms associated with pressure transmitted through the fluid. As lubricant film decreases, λ decreases. For the initiation of fluid film lubrication failure, Bayer (1994) mentions a limit λ value of 3; Neale (1997) estimates it as 5. Some mechanical parts can operate under lower λ values. Mixed lubrication, also called partial-elastohydrodynamic lubrication (partial-EHL), occurs when λ value is in the 1 to 3 range. In this regime, contacts between the asperities are expected to occur; then, wear takes place due to physical interaction of both solid surfaces.

Depending on thermal effects and localized pressure peaks, film breakdown occurring at higher asperities may give origin to severe wear, such as scuffing. When λ value is smaller than unity, oil film thickness is very small, not fluid anymore, being then related to boundary lubrication regime, where both wear and friction are likely to achieve high values, unless boundary lubricants are used (Hutchings, 1992).

Despite seen in literature to a great extent, the use of λ value to analyze wear and friction responses is considered somewhat inconsistent by Cann and coworkers (1994), because some microscopic effects, such as the micro-elastohydrodynamic lubrication at the asperities, cannot be explained through λ value. Same observation is done on the use of ηV/W factor (Luengo, Israelachvili and Granick, 1996).

A similar way to characterize lubrication regimes is by the lubrication number (ηV)/(Pσ), where η is the oil viscosity, V the sliding velocity, P the mean contact pressure and σ the equivalent roughness. The (ηV)/(Pσ) parameter is similar to the λ factor, since ηV/P is proportional to the fluid film thickness (Bayer, 1994). According to Dizdar and Andersson, (1997), it was studied by Schipper in 1990's, whose observations indicated the (ηV)/(Pσ) factor is a more realistic variable to use for categorization of wear regimes, and thus the lubrication modes, than the more widely used λ factor. Jisheng and Gawne (1997) also used this factor in their studies of lubrication regimes of sliding systems. Anyway, parameters often used in Stribeck diagram denote that friction and, consequently, wear in lubricated conditions depend mostly on load and velocity. This was explored in the present paper in order to verify it as a factor of identification of distinct wear and friction trends.

Another way to characterize tribological response of rubbing contacts, concerning especially wear, is the Archard equation. It is seen in literature for lubricated sliding wear modeling (Ting and Mayer, 1974; Tomanik, 2000) and states that wear in volume is proportional to load and to sliding distance, and inversely proportional to material hardness (Hutchings, 1992). A wear coefficient, k, is obtained from Archard equation. According to Ting and Mayer (1974), for lubricated tribopairs such as the piston ring-cylinder bore tribopair, it is postulated that wear occurs when a given minimum value of lubricant film thickness, around 1 μm, is attained. This postulation could allow extrapolation for wear occurrence in other tribopairs, considering the respective surface equivalent roughness and its relationship with a minimum film thickness. Hutchings (1992), based on Czichos and Habbig work (1984), described the wear coefficient k as a function of λ factor and the lubrication regimes. This is seen in Fig. 2, where k varies from 10^{-4} to 10^{-10} $mm^3/(Nm)$ from boundary to full film lubrication regime.

In the present paper, the behavior of friction and wear in lubricated sliding system is discussed considering Stribeck diagram. The use of Archard expression is also discussed. Friction and wear results were obtained from sliding tests, performed by varying the loading level, the type of sliding motion and lubricant characteristics.

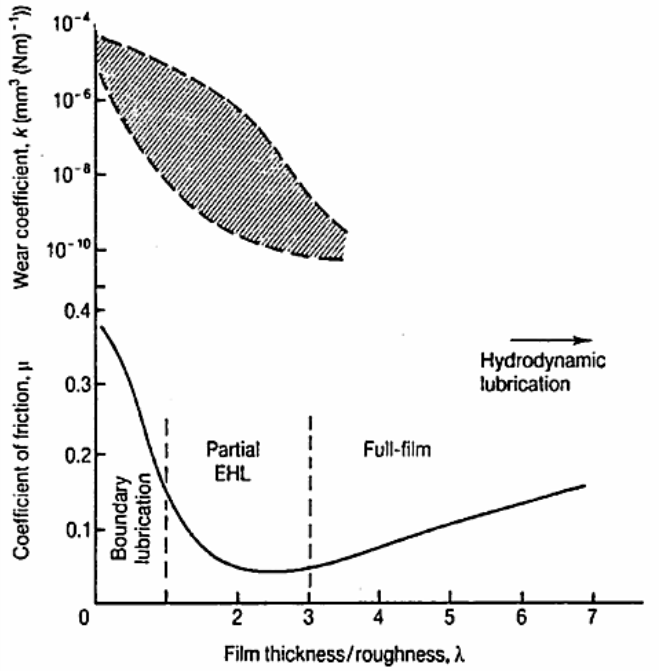

Figure 2. Lubrication regimes and wear coefficient in sliding of metals, as a function of λ (reproduced from Hutchings, 1992).

Materials and Methods

Sliding tests were performed through a TE67 Plint & Partners rig with rotating pin-on-disk (code D) and reciprocating pin-on-plate (code P) configurations. In both systems, normal load is pneumatically applied on the pin. The contact between the pin and the counter-body is immersed in oil bath, heated to 100 ºC. The equipment is able to control the load, the oil bath temperature and the disk rotational speed, or plate oscillation frequency. The friction force between the specimens is monitored during the tests. The measured values can be stored in data files; in the tests, the data acquisition rate was 0.1 Hz. Every test was run with a previous step of 1,200 s (0.33 h) without loading at the test velocity, for oil heating up to 100 ºC. After the previous step, load was applied. The test was stopped after completing 50,000 pin cycles on the disk, or 100,000 pin cycles on the plate. Two loading levels were selected, based on the average sliding velocity to normal load ratio (V/W). The tests with mild loading level were coded as PP and DD tests and the severe loading as P and D. Table 1 summarizes the test conditions. According to IRG (International Research Group) diagram, which roughly indicates the transition among lubrication regimes based on load and velocity values (Gee, Begelinger, and Salomon, 1984), the test conditions were under mixed lubrication condition, as shown in Fig. 3.

Table 1. Summary of the testing conditions.

Test	Temperature, ºC	Load W, N	Speed, rpm (Frequency, Hz)	Stroke radius, mm	Average velocity V_{med}, m/s	Mechanical loading (V/W)	Distance, m	Time, h	Cycles
DD	100	80	184 (3.1)	22	0.42	Mild	6,912	4.5	50,000
PP	100	80	250 (4.2)	16 (*)	0.27	Mild	3,200	3.3	100,000
D	100	283	184 (3.1)	11	0.21	Severe	3,456	4.5	50,000
P	100	283	250 (4.2)	8 (*)	0.13	Severe	1,600	3.3	100,000

Obs.: D, DD: rotating tests; P, PP: reciprocating tests; (*) This value is related to the ½ stroke in the reciprocating motion

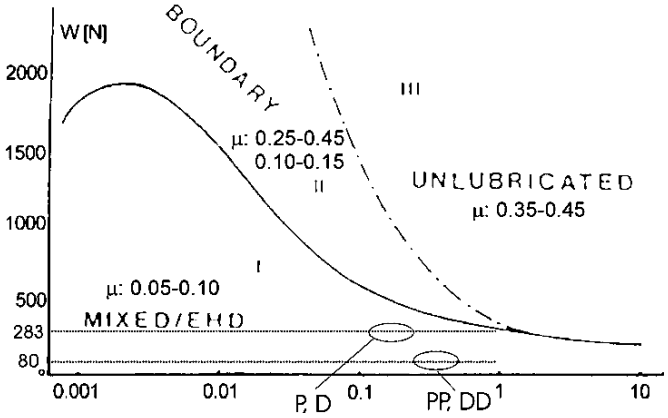

Figure 3. IRG Diagram (Gee, Begelinger, and Salomon, 1984) showing the test conditions.

Pin specimens were of AISI 52100 steel, 63 HRc hardness, with 5.5 ± 0.3 mm radius rounded test surface. Ra (mean height of asperities) roughness of test surface was 0.51 ± 0.05 μm (1.25 mm measurement length). Disks and plates were of AISI 8640 steel, quenched and tempered to 48 HRc hardness. Ra roughness of disks was 0.65 ± 0.15 μm and plates had 1.3 ± 0.2 μm. Further details of specimens are described elsewhere (Maru and Tanaka, 2006).

Quartz (SiO_2) was used as abrasive contaminant, having average hardness of 1,000 HV and 15 μm average particle size. Abrasive concentration in oil was 0.5 mg/ml.

As lubricants, paraffin base oils were used, one with and another without additives. Both oils were commercial, of same viscosity index (VI 100), and normally recommended for gearbox lubrication. In the oil with additives, optical spectrometry analysis indicated phosphorus presence. Through infra-red spectrometry, sulfur was also detected in its composition. SA code was used for the tests with oil without additive; CA for the tests with additive in oil.

Table 2 shows the codes used for the 16 sliding conditions tests. At least three tests were run for each test condition.

Analyses on the worn surfaces were performed by optical microscope. The worn profiles were measured from a Kosaka profilometer. Unless mentioned, all shown profiles were taken transversal to sliding direction.

Table 2. Codification used for the sliding tests.

Code	Loading	Additive	Contaminant	System
PP SA	Mild	No	No	Reciprocating
DD SA	Mild	No	No	Rotating
P SA	Severe	No	No	Reciprocating
D SA	Severe	No	No	Rotating
PPc SA	Mild	No	Yes	Reciprocating
DDc SA	Mild	No	Yes	Rotating
Pc SA	Severe	No	Yes	Reciprocating
Dc SA	Severe	No	Yes	Rotating

Code	Loading	Additive	Contaminant	System
PP CA	Mild	Yes	No	Reciprocating
DD CA	Mild	Yes	No	Rotating
P CA	Severe	Yes	No	Reciprocating
D CA	Severe	Yes	No	Rotating
PPc CA	Mild	Yes	Yes	Reciprocating
DDc CA	Mild	Yes	Yes	Rotating
Pc CA	Severe	Yes	Yes	Reciprocating
Dc CA	Severe	Yes	Yes	Rotating

Results

Microscopic morphology of worn surfaces is shown elsewhere (Maru and Tanaka, 2006). It was shown that the loading level strongly affected pin wear, even though both loading conditions were under same mixed lubrication. The type of system motion was also very influencing on pin wear, being observed more wear when the reciprocating motion was used. The presence of additive and contaminant in oil acted in opposite way, as expected. The task is then to verify if these distinct effects, previously verified through analyses of worn surfaces of the pins, can be detected through the use of Archard equation and Stribeck diagram. Before showing these analyses, some considerations concerning profilometry results were made.

Worn Profiles of Tested Specimens

Measurements of worn profiles of both pin and counter-body tested specimens have shown distinct wear levels in each test condition. Figure 4 shows pin worn surface profiles from reciprocating tests under mild loading level. Analyses on pin worn profiles resulting from the corresponding rotating tests had similar results.

From Fig. 4, it is noticed that, as expected, without additives in the oil (PP SA and PPc SA), pin surface flattened as a consequence of wear and, when contaminated oil was used, wear was even more accentuated. With additive containing oil (PP CA and PPc CA), flattening was apparent only when contaminated oil was used.

Regarding the counter-bodies tested under mild loading level, wear was only in terms of some smoothening at surface asperities. As an example, Fig. 5 shows a plate surface tested under PPc CA condition. Similar smoothening was noticed in the disks.

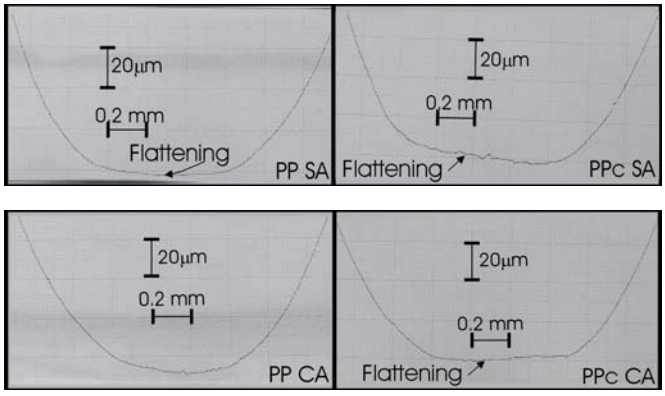

Figure 4. Pin worn profiles after reciprocating tests under mild loading. Sliding direction normal to sheet.

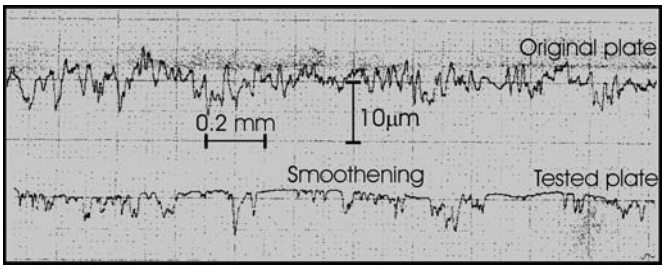

Figure 5. Profiles of a plate before and after test (PPc CA), taken parallel to the sliding direction.

Under severe loading condition, the resulting wear was obviously more prominent. Groove occurred in the counter-bodies;

its intensity depended on the test condition. Figure 6 shows the results for reciprocating tests, P SA and P CA. Pronounced grooving is noticed in both plates, being that additive in oil suppressed roughening of the worn surfaces.

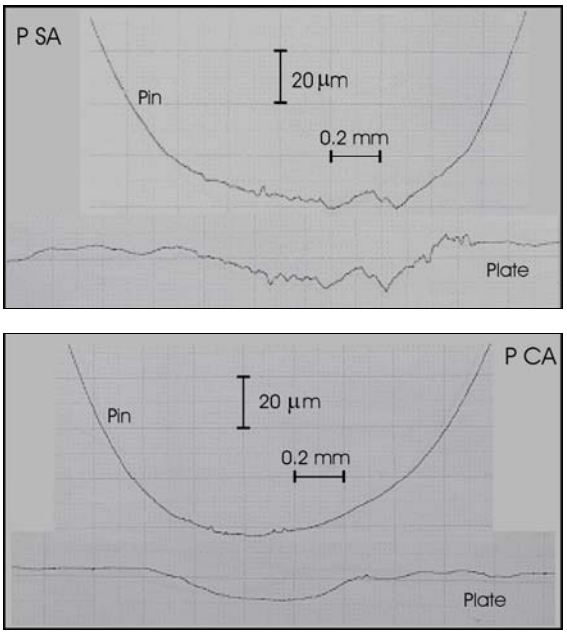

Figure 6. Surface profiles of tested specimens (P SA and P CA tests).

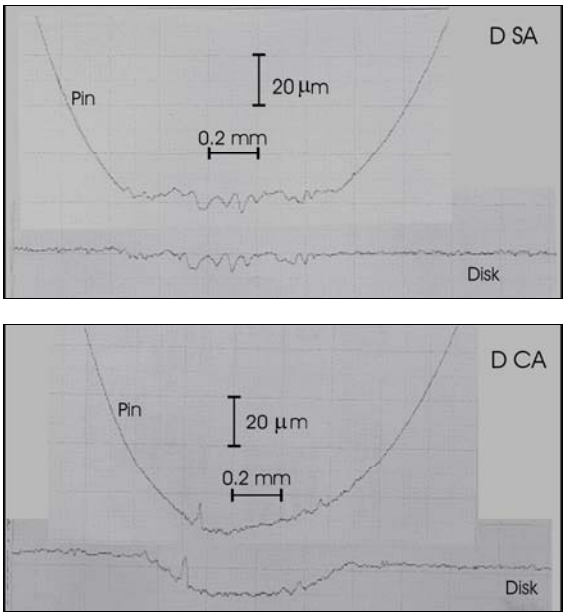

Figure 7. Surface profile of tested specimens (D SA and D CA tests).

The worn profiles resulting from rotating tests under severe loading have shown slight differences from those seen in Fig. 6. Figure 7 shows the results. It is noticed that, without additive in oil, severe roughening occurred with pronounced material loss of pin. In the same Figure, it is observed that the use of oil with additive has inhibited surface roughening and apparently decreased pin wear; however, surprisingly, the disk has undergone pronounced grooving.

Observing the results of CA tests in Fig. 6 and 7, it is noticed that roughening in additive containing oil tests was dependent on the system type. Roughening was observed only in rotating system. Differences in oil flux among the tested systems were considered as cause of distinct wear, being that interaction of particles in the contact area, together with oil flushing intensity, may affect tribofilm formation, as pointed out by Bayer (1994). This is discussed elsewhere (Maru and Tanaka, 2006).

In terms of contaminant effect in the tests under severe loading, it was not significant. It is seen when Fig. 6 and 7 are compared to Fig. 8 and 9, being apparent that the severe loading level reduced possibility of contaminant penetration into the contact area.

Observing all worn profiles of severe loading tests, it is possible to see that most of the grooves originated from the rubbing fit on one another. This fact suggests a mechanism similar to ploughing, as described by Wang and coworkers (1991) as a wear mechanism of lubricated tests.

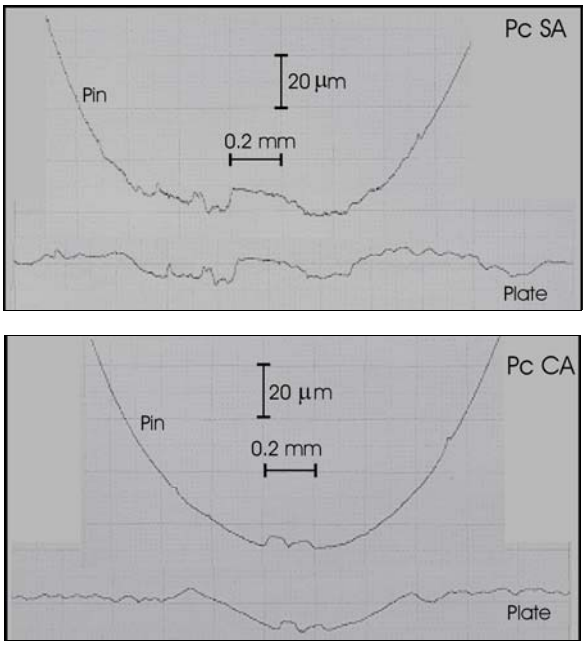

Figure 8. Surface profile of tested specimens (Pc SA and Pc CA tests).

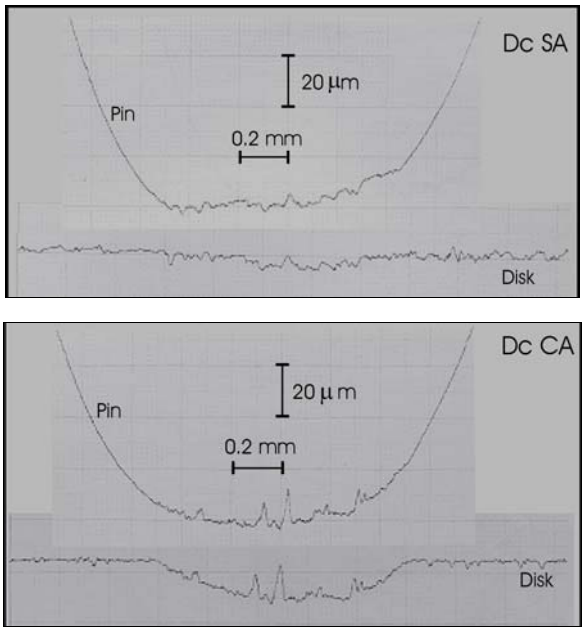

Figure 9. Surface profile of tested specimens (Dc SA and Dc CA tests).

Wear Coefficient "k"

According to Archard expression, the wear coefficient k relates the volumetric wear rate with the applied load and the sliding distance (Hutchings, 1992), given by Eq. 1.

$$Q = k \cdot W \cdot \Delta S \quad (1)$$

Where:
Q: volumetric wear [mm^3] of the lower hardness body
k: wear coefficient [$mm^3/(m.N)$]
W: normal load [N]
ΔS: sliding run distance [m]

The k value of Archard equation is useful for comparing wear rates of different materials (Hutchings, 1992).

In the present work, k can be calculated for evaluation of resulting wear from the different test conditions. Since k is related to wear of the material of lower hardness, approximate wear volume values of the counter-bodies can be used. In order to know the k value resulting from the performed tests, wear volumes were obtained by approximate calculations. Since profilometry analyses have shown that wear of counter-body was noticeable only in severe loading tests (P and D), k is obtainable only for these test conditions. Therefore, a maximum k value of the performed tests can be calculated. So as to determine wear volume of counter-bodies tested in P and D conditions, the maximum transversal worn was measured from the profilometry results. The transversal area of a disk tested in D CA condition had a measured magnitude around 0.008 mm^2, as shown in Fig. 10 (hatched area A). Considering this magnitude as the maximum transversal worn area of the counter-bodies tested in P and D conditions, the maximum wear coefficient k can be calculated, as shown in Fig. 11. Simplified geometries were taken into consideration in order to simplify calculations.

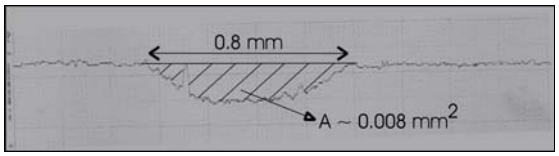

Figure 10. Surface profile of a disk after D CA test.

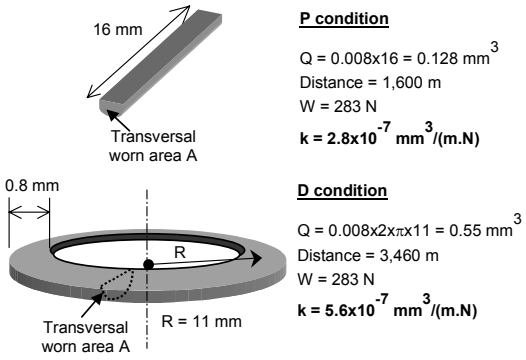

Figure 11. Geometrical estimates for the calculation of counter-body wear volume and the wear coefficient k for P and D test conditions.

Both k values were in the order of 10^{-7} $mm^3/(N.m)$. As expected, they correspond to mixed lubrication according to the k ranges by Czichos and Habig (1984) (seen in Fig. 2).

How wear coefficient is changed by the studied influences can be alternatively analyzed by considering another wear coefficient, very similar to k. It was identified as wear coefficient k' [$\mu m^2/(N.m)$]. Instead of wear volume, k' value takes into account the measurement of top view area of the pins affected by wear, by unity of load and sliding distance. The area of the pins affected by wear was considered normalized by run distance, as shown in Eq. 2. Values of normalized wear-affected area of pins of all test conditions are shown in Fig. 12 and Fig. 13 shows the corresponding k' values.

$$k' = Q'/ W \cdot \Delta S, \text{ or } k' = \text{normalized area } /W \quad (2)$$

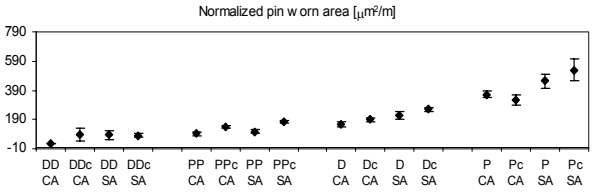

Figure 12. Values of pin worn area of the tested conditions, normalized by run distance.

Figure 13 evidences that the wear coefficient k' has no correlation with overall evolution of pin wear shown in Fig. 12. Then, k' value, despite its similarity to the wear coefficient k of Archard equation, was not able to adequately characterize overall wear behavior in the performed lubricated sliding tests. On the other hand, if one takes each series in separate, it is possible to see that k' evidence the distinct effects on wear of additive and contamination in oil.

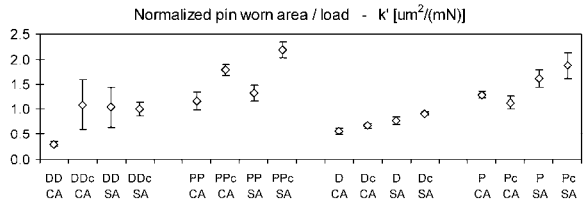

Figure 13. Wear coefficient k', calculated as normalized pin worn area divided by load.

Stribeck Diagram

Schematic diagram showing relationships among wear, friction and film thickness, is presented in Fig. 14, from Bayer (1994). This Figure also highlights region of mixed lubrication, where both wear and friction are supposed to go down as the film thickness increases.

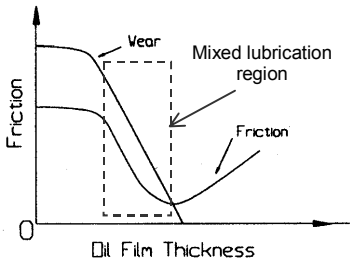

Figure 14. Schematic diagram relating oil film thickness to wear and friction (adapted from Bayer, 1994).

As previously described (Bayer, 1994; Hutchings, 1992), oil film thickness is affected by the $\eta V/W$ factor, where η is the oil viscosity, V (or V_{med}) the average sliding velocity and W the normal load. In the performed tests, oil viscosity can be considered as constant; therefore, it is thought that variations in oil film thickness are roughly related to V/W ratio. Concerning the V/W ratios in the performed tests, values decrease following the order DD-PP-D-P. In

this case, the average values of pin wear increase, being in accordance to behavior estimated in Fig. 14. This is better shown in Fig. 15(a). Other parameters similar to V/W ratio are usually applied in Stribeck diagram; one of them is the $(\eta V)/(P\sigma)$ factor, by Dizdar and Andersson (1997). When applying it in the present study, change was minimum, as can be seen by comparing Fig. 15(a) to Fig. 15(b). The σ parameter was calculated as $\sigma = (Ra_1^2 + Ra_2^2)^{1/2}$, where Ra_i is the mean height of asperities of i surface.

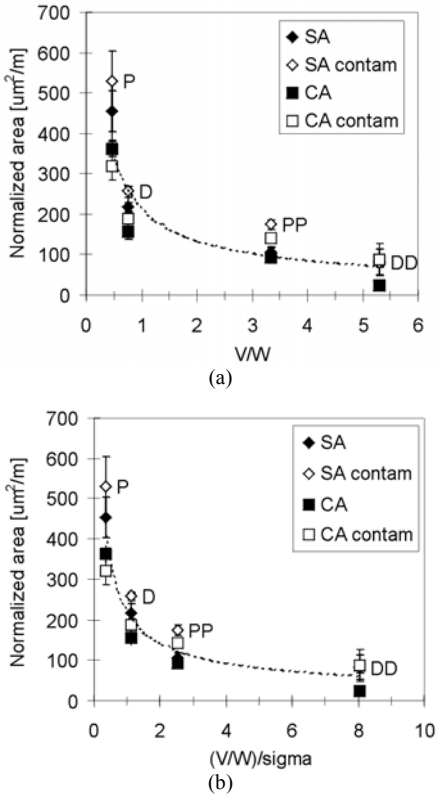

Figure 15. Normalized pin worn area as a function of (a) V/W; (b) (V/W)/σ.

An observation to be made is that, in both charts, all results can be fit in only one curve. The already known differences in wear, for instance, among both used mechanical devices, are not perceived. In truth, the right side chart even enhances tendency to all series, P-D-PP-DD, to follow only one logarithmic trend.

Alternatively, the minimum EHL oil film thickness, h, considering ball-on-flat contact geometry, should follow the expression cited by Hutchings (1992), rewritten in Eq. 3:

$$h = 1{,}79 \cdot \alpha^{0,49} \cdot (\eta_0 \cdot V)^{0,68} \cdot R^{0,47} \cdot W^{-0,07} \cdot E'^{-0,12} \quad (3)$$

where:

η_o: oil viscosity in atmospheric pressure [cP], or [10^{-3} Pa.s]

R: equivalent contact radius [m], with $1/R = 1/R_1 + 1/R_2$ and R_i = i body contact radius (i = 1..2, with reference to the contacting bodies)

E': equivalent elastic modulus [Pa], with $1/E' = (1-\nu_1^2)/E_1 + (1-\nu_2^2)/E_2$; where ν_i = Poisson coefficient of i body and Ei = elastic modulus of i body (i = 1..2)

α: coefficient of oil viscosity in $\eta = \eta_0 e^{(\alpha P)}$, P being the hydrostatic pressure. For mineral oils:

$\alpha \sim (0.6 + 0.965 \log_{10} \eta_0).10^{-8}$ (Hutchings, 1992)

Premise of Eq. 3 is the use of Reynolds hydrodynamic lubrication and Hertz elasticity theories (Hutchings, 1992; Dowson, 1997 and others). It shows exponents of 0.68 for V and –0.07 for W, from which a $V^{0,68}/W^{0,07}$ factor is suggested for wear behavior analysis. The same factor including roughness consideration was also analyzed. Figure 16 shows the resulting diagrams. In the same way as previous ones, single relationship is clearly observed between $V^{0,68}/W^{0,07}$ factor and wear (Fig.16(a)), being the curves very similar for all oil variations studied. More than that, the use of EHL exponents emphasized that all the tested conditions follow a single lubrication trend. So far, all diagrams suggest that lubrication changed in a continuous way, does not mattering the physical differences in the test conditions. However, when roughness was considered (Fig. 16(b)), single wear trend is not observed any more; now, differences in wear trend among both tested systems are evidenced. Also, the diagram in Fig. 16(b) can indicate that lubrication in pin-on-plate tests was more critical. Nevertheless, distinctions in wear behavior in terms of variations in oil (contamination and additive presence) cannot still be evidenced.

One consideration to be discussed is the use of initial roughness values to plot the diagrams. Worn profile analyses have shown that topography geometry changes to a great extent after being submitted to rubbing process. Mainly in the severe loading tests, it was noticed that the surface roughness had completely changed the orientation of the grooves after sliding test (Maru and Tanaka, 2006). Then, consideration of initial roughness in the diagram can only indicate the lubrication condition in the initial sliding period, commonly denominated running-in. Besides that, those exponents seen in Eq.3 in load and velocity parameters is related to a ball-on-flat contact, what is completely changed along the sliding test. It confirms that the trend curves seen in the diagram of Fig. 16(b) can be related to the lubrication condition at initial stage. In other words, it can be an indication that the wear performance is in fact defined at early stages.

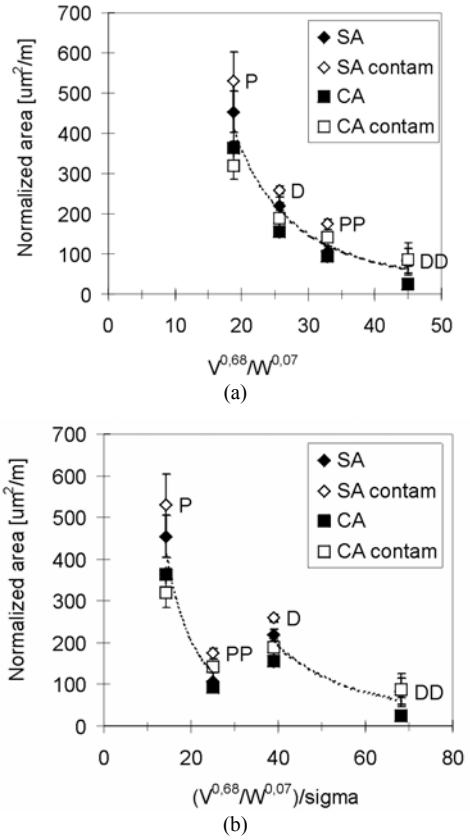

Figure 16. Normalized pin worn area as a function of (a) $V^{0,68}/W^{0,07}$; (b) $(V^{0,68}/W^{0,07})/\sigma$.

On the other hand, Stribeck diagrams are mostly used with friction coefficient values instead of wear in order to characterize lubrication. However, plotting the average values of friction coefficient resulting from the tests, as a function of the studied factors, absence of global relationships is evident, as seen in Fig. 17. Alternatively, Fig. 17(d) seemed to display some distinct friction trend among the rotating and reciprocating devices.

Observations resulting from the analyses of wear and friction coefficient through the $(V^{0,68}/W^{0,07})/\sigma$ factor evidenced distinction in lubrication trend among the tested devices, as expected. It was related to the early sliding stage.

Concluding Remarks

Wear coefficient k', obtained by considering worn area, was not able to adequately characterize overall wear behavior in the performed lubricated sliding tests. On the other hand, if load and velocity are kept constant, the effect on wear of additive and contamination in oil can be evidenced in k'.

When wear and friction coefficient were considered as a function of $(V^{0,68}/W^{0,07})/\sigma$ factor related to the early sliding stage, distinction in lubrication trend among the tested devices was possible to be evidenced.

Acknowledgements

The authors express thanks to FAPESP for the grant (project no. 97/12753-9) and to INA Rolamentos Ltda. for pin specimens supply.

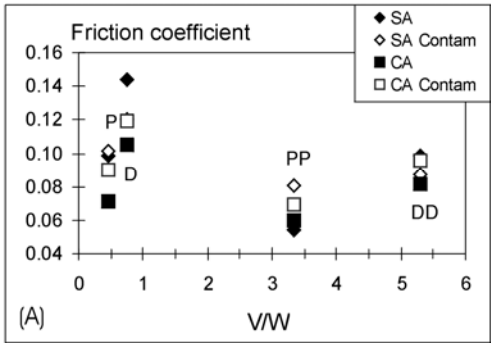

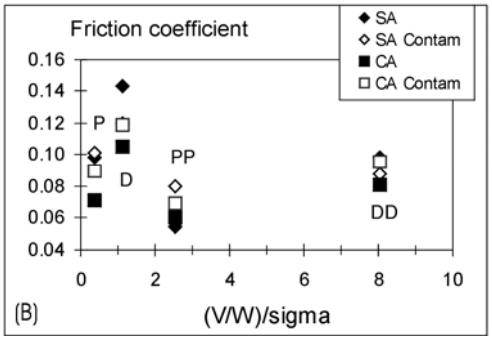

Figure 17. Average values of friction coefficient as a function of the studied factors. (a) V/W, (b) (V/W)/σ, (c) $V^{0,68}/W^{0,07}$ and (d) $(V^{0,68}/W^{0,07})/\sigma$.

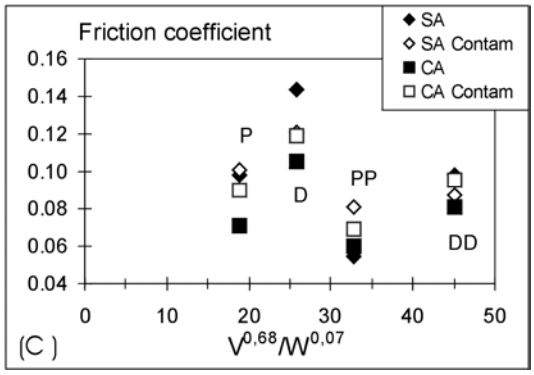

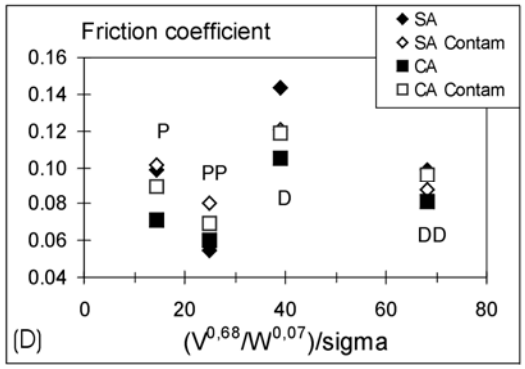

Figure 17. (Continued).

References

Bayer, R.G., 1994, "Mechanical Wear Prediction and Prevention", Marcel Dekker, USA, 657 pp.

Cann, P., Ioannides, E., Jacobson, B., and Lubrecht, A.A., 1994, "The lambda ratio – a critical re-examination", Wear, Vol.175, pp. 177-188

Cheng, H.S., 1988, "Elastohydrodynamic lubrication", In: CRC Handbook of Lubrication - Theory & Design, CRC Press, pp. 139-162

Czichos, H., and HABIG, K.-H., 1984, "Lubricated wear of metals", In: Proceedings of the 11th Leeds-Lyon Symposium on Tribology, Butterworths, England, pp.135-147

Dizdar, S., and Andersson, S., 1997, "Influence of pre-formed layers on wear transition in sliding lubricated contacts", Wear, Vol.213, pp. 117-122

Dowson, D., 1995, "Elastohydrodynamic and micro-elastohydrodynamic lubrication", Wear, 190, pp. 125-138

Dowson, D., 1997, "History of Tribology", Professional Engineering Publishing, UK, 759 pp.

Gee, A.W.J., Begelinger, A., and Salomon, G., 1984, "Failure mechanisms in sliding lubricated contacts", In: Mixed lubrication and lubricated wear, Proceedings of the 11th Leeds-Lyon Symposium, Butterworths, England, pp.108-116

Hutchings, I.M., 1992, "Tribology: friction and wear of engineering materials", Edward Arnold, Great Britain, 273 pp.

Jisheng, E., and Gawne, C.T., 1997, "Wear characteristics of plasma-nitrided CrMo steel under mixed and boundary conditions", Journal of Materials Science, Vol.32, pp. 913-920

Ludema, K.C., 1996, "Friction, Wear, Lubrication: a Textbook in Tribology", CRC Press, USA, 257 pp.

Luengo, G., Israelachvili, J., and Granick, S., 1996, "Generalized effects in confined fluids: new friction map for boundary lubrication", Wear, Vol.200, pp. 328-335

Maru, M.M., and Tanaka, D.K. 2006, "Influence of loading, contamination and additive on the wear of a metallic pair under rotating and reciprocating lubricated sliding". Journal of The Brazilian Society of Mechanical Sciences Vol.28, No.3, pp. 278-285.

Neale, M.J., 1997, "The Tribology Handbook", 2nd Ed., USA, Butterworth-Heinemann

Ting, L.L., and Mayer Jr, J.E., 1974, "Piston ring lubrication and cylinder bore wear analyses, Part II – Theory verification", Journal of Lubrication Technology, Transactions of the ASME, pp. 258-266

Tomanik, A.E., 2000, "Modelamento do desgaste por deslizamento em anéis de pistão de motores de combustão interna", PhD Thesis, Universidade de São Paulo, Brazil, 198 pp.

Wakuri, Y., Soejima, M., Kitahara, T., Fujisaki, K., and Nuki, K., 1995, "Effect of lubricating oils on piston ring friction and scuffing", Japanese Journal of Tribology, Vol.40, No.5, pp. 437-449

Wakuri, Y., Soejima, M., Yamamoto, T., and Ootsubo, M., 1988, "Fundamental studies on scuffing between cylinder and piston ring", International Journal of Vehicle Design, Vol.9, No.2, pp. 203-215

Wang, F-X., Lacey, P., Gates, R.S., and Hsu, S.M., 1991, "A study of the relative surface conformity between two surfaces in sliding contact", Journal of Tribology, Transactions of the ASME, Vol.113, pp. 755-761